Received: 23 August 2023 | Revised: 25 January 2024 | Accepted: 10 February 2024

DOI: 10.1002/pld3.573

RESEARCH ARTICLE

Light quality-dependent roles of REVEILLE proteins in the circadian system

Cassandra L. Hughes[1] | Yuyan An[2] | Julin N. Maloof[1] | Stacey L. Harmer[1]

[1]Department of Plant Biology, University of California, Davis, Davis, California, USA

[2]College of Life Sciences, Shaanxi Normal University, Xi'an, China

Correspondence
Stacey L. Harmer, Department of Plant Biology, University of California, Davis, Davis, CA 95616, USA.
Email: slharmer@ucdavis.edu

Funding information
U.S. Department of Agriculture-National Institute of Food and Agriculture, Grant/Award Number: CA-D-PLB-2259-H; National Institutes of Health, Grant/Award Number: R01 GM069418

Abstract

Several closely related Myb-like activator proteins are known to have partially redundant functions within the plant circadian clock, but their specific roles are not well understood. To clarify the function of the *REVEILLE 4*, *REVEILLE 6*, and *REVEILLE 8* transcriptional activators, we characterized the growth and clock phenotypes of CRISPR-Cas9-generated single, double, and triple *rve* mutants. We found that these genes act synergistically to regulate flowering time, redundantly to regulate leaf growth, and antagonistically to regulate hypocotyl elongation. We previously reported that increasing intensities of monochromatic blue and red light have opposite effects on the period of triple *rve468* mutants. Here, we further examined light quality-specific phenotypes of *rve* mutants and report that *rve468* mutants lack the blue light-specific increase in expression of some circadian clock genes observed in wild type. To investigate the basis of these blue light-specific circadian phenotypes, we examined RVE protein abundances and degradation rates in blue and red light and found no significant differences between these conditions. We next examined genetic interactions between *RVE* genes and *ZEITLUPE* and *ELONGATED HYPOCOTYL5*, two factors with blue light-specific functions in the clock. We found that the *RVEs* interact additively with both *ZEITLUPE* and *ELONGATED HYPOCOTYL5* to regulate circadian period, which suggests that neither of these factors are required for the blue light-specific differences that we observed. Overall, our results suggest that the *RVEs* have separable functions in plant growth and circadian regulation and that they are involved in blue light-specific circadian signaling via a novel mechanism.

KEYWORDS
Arabidopsis thaliana; blue light; flowering time; hypocotyl elongation; *RVE4*, *RVE6*, *RVE8*

1 | INTRODUCTION

The circadian clock provides a time-keeping mechanism to predict daily and seasonal changes. Circadian components also regulate physiological outputs, such as plant growth and photoperiodic regulation of flowering (Maeda & Nakamichi, 2022; Seluzicki et al., 2017; Song et al., 2015), and help increase an organism's fitness by ensuring it is well-adapted to its environment (Dodd et al., 2005; Ouyang et al., 1998; Spoelstra et al., 2016). These biological rhythms have a period of approximately 24 h and persist in a constant environment (Creux & Harmer, 2019).

While circadian rhythms continue in the absence of environmental signals, the circadian system is sensitive to a variety of environmental cues. Abrupt changes in light and temperature can reset clock

phase, and in addition, changes in light intensity and temperature can affect the free-running pace of the circadian oscillator (Creux & Harmer, 2019). In plants, as in most diurnal organisms, increased light intensity shortens circadian period, while in most nocturnal organisms, increased light intensity causes period lengthening (Aschoff, 1979). This general relationship is termed "Aschoff's rule" and is speculated to underlie appropriate entrainment, which matches circadian phase with the environment (Oakenfull & Davis, 2017; Sanchez et al., 2020).

In eukaryotes, the circadian system is made up of multiple interacting transcriptional feedback loops. Most plant circadian clock components are repressors of transcription (Hsu & Harmer, 2014). However, several transcriptional activators have been identified. *REVEILLE 4* (*RVE4*), *REVEILLE 6* (*RVE6*), and *REVEILLE 8* (*RVE8*) are the primary known transcriptional activators within the plant circadian clock and act partially redundantly with each other. These *RVEs* are responsible for activating expression of afternoon and evening-phased genes, including *TIMING OF CAB EXPRESSION 1* (*TOC1*), the related *PSEUDO-RESPONSE REGULATOR* genes (*PRR5*, *PRR7*, and *PRR9*), and the evening complex genes *EARLY FLOWERING 3* (*ELF3*), *EARLY FLOWERING 4* (*ELF4*), and *LUX ARRHYTHMO* (*LUX*) (Farinas & Mas, 2011; Hsu et al., 2013; Rawat et al., 2011). Acting in opposition to the *RVEs* are the related Myb-like transcription factors *CIRCADIAN CLOCK ASSOCIATED 1* (*CCA1*) and *LATE ELONGATED HYPOCOTYL* (*LHY*), which repress these same targets (Adams et al., 2018; Alabadi et al., 2001; Hazen et al., 2005; Kamioka et al., 2016; Li et al., 2011; Nagel et al., 2015). Together, *CCA1*, *LHY*, *RVE4*, *RVE6*, and *RVE8* increase robustness of circadian rhythms and regulate clock pace (Shalit-Kaneh et al., 2018).

Studies conducted over the past 20 years have led to considerable insight into how light signaling components interact with the circadian machinery. Phytochromes, which are red light photoreceptors, can affect circadian period and are known to physically interact with the ELF3 protein (Oakenfull & Davis, 2017). Multiple blue light photoreceptors influence the clock, including cryptochromes and the F-box protein ZEITLUPE (ZTL). CRYPTOCHROME2 (CRY2) physically interacts with PRR9 to repress its activity (He et al., 2022). ZTL also inhibits the function of PRR proteins by promoting the degradation of TOC1 and PRR5 in a blue light-dependent manner (Fujiwara et al., 2008; Más et al., 2003). In addition to the photoreceptors, downstream light signaling components connect light inputs to the circadian clock. For example, *ELONGATED HYPOCOTYL 5* (*HY5*) is a transcription factor that acts downstream of multiple types of photoreceptors and also affects circadian clock function (Gangappa & Botto, 2016; Xiao et al., 2022). Binding of HY5 to its targets, including clock gene promoters, is promoted by blue light (Hajdu et al., 2018). This leads to an enhanced short-period phenotype of *hy5* mutants in blue light compared with red light (Hajdu et al., 2018).

The study of light responses in controlled environmental conditions has revealed both inhibitory and synergistic interactions between light signaling pathways (Guo et al., 1998; Más et al., 2000; Oakenfull & Davis, 2017). Many circadian assays are performed in constant white or red plus blue light conditions, but separately examining the effects of monochromatic red and monochromatic blue light may uncover more detailed interactions between the clock and light input pathways. The *rve4-1 rve6-1 rve8-1* triple mutant was initially characterized as having a long period in constant red plus blue light conditions, a proxy for natural white light (Hsu et al., 2013). Subsequent experiments found that the period of *rve4-1 rve6-1 rve8-1* is consistently longer than wild type in both monochromatic red and monochromatic blue light but that the response of period to light intensity differs from wild type specifically in blue light (Gray et al., 2017). In red light, the period of both wild type and *rve4-1 rve6-1 rve8-1* shortens as the fluence rate increases. However, while the period of wild-type plants also decreases under increasing intensities of blue light, the period of *rve4-1 rve6-1 rve8-1* mutants lengthens (Gray et al., 2017). This change in responsiveness between monochromatic red and monochromatic blue light suggests that *RVE4*, *RVE6*, and *RVE8* may be involved in light quality-specific circadian regulation.

We wanted to further investigate light quality-specific roles of *RVE4*, *RVE6*, and *RVE8* within the plant circadian system. However, we found that previously generated T-DNA alleles within the *rve4-1 rve6-1 rve8-1* triple mutant have regained significant *RVE* gene expression (Shalit-Kaneh et al., 2018). To circumvent this problem, we generated new *rve* alleles using CRISPR-Cas9 (Hughes & Harmer, 2023). Here, we report the characterization of single, double, and triple mutants containing CRISPR-Cas9-generated alleles of *RVE4*, *RVE6*, and *RVE8*. We assessed the phenotypes of these new mutants in monochromatic red and monochromatic blue light and found blue light-specific phenotypes similar to those observed in the T-DNA *rve468* mutant. We then investigated whether differences in RVE protein abundance or interactions with light quality-specific factors could account for the observed light quality-specific differences in *rve468* mutants. We find that RVE protein abundance and degradation rates are not different between monochromatic red and monochromatic blue light. We also find that interactions between *RVE4*, *RVE6*, *RVE8*, and *ZTL* or *HY5* are likely not responsible for the blue-specific phenotypes of *rve468* mutants. These data suggest that the RVEs interact with novel blue-specific signaling factors to influence circadian clock function in a light quality-specific manner.

2 | RESULTS

2.1 | Synergistic, additive, and epistatic interactions between *rve* genes in control of plant growth

We used CRISPR-Cas9 technology with multiple guide RNAs to generate a novel *rve4 rve6 rve8* triple mutant (Hughes & Harmer, 2023). A line with frameshift mutations predicted to cause premature stop codons in all three genes was selected and named *rve4-11 rve6-11 rve8-11* (Figure 1a). The premature stop codon is upstream of the Myb-like DNA-binding domain in *RVE4*, downstream of the Myb-like DNA-binding domain but within the adjacent conserved proline-rich region in *RVE6*, and upstream of the conserved C-terminal domain in

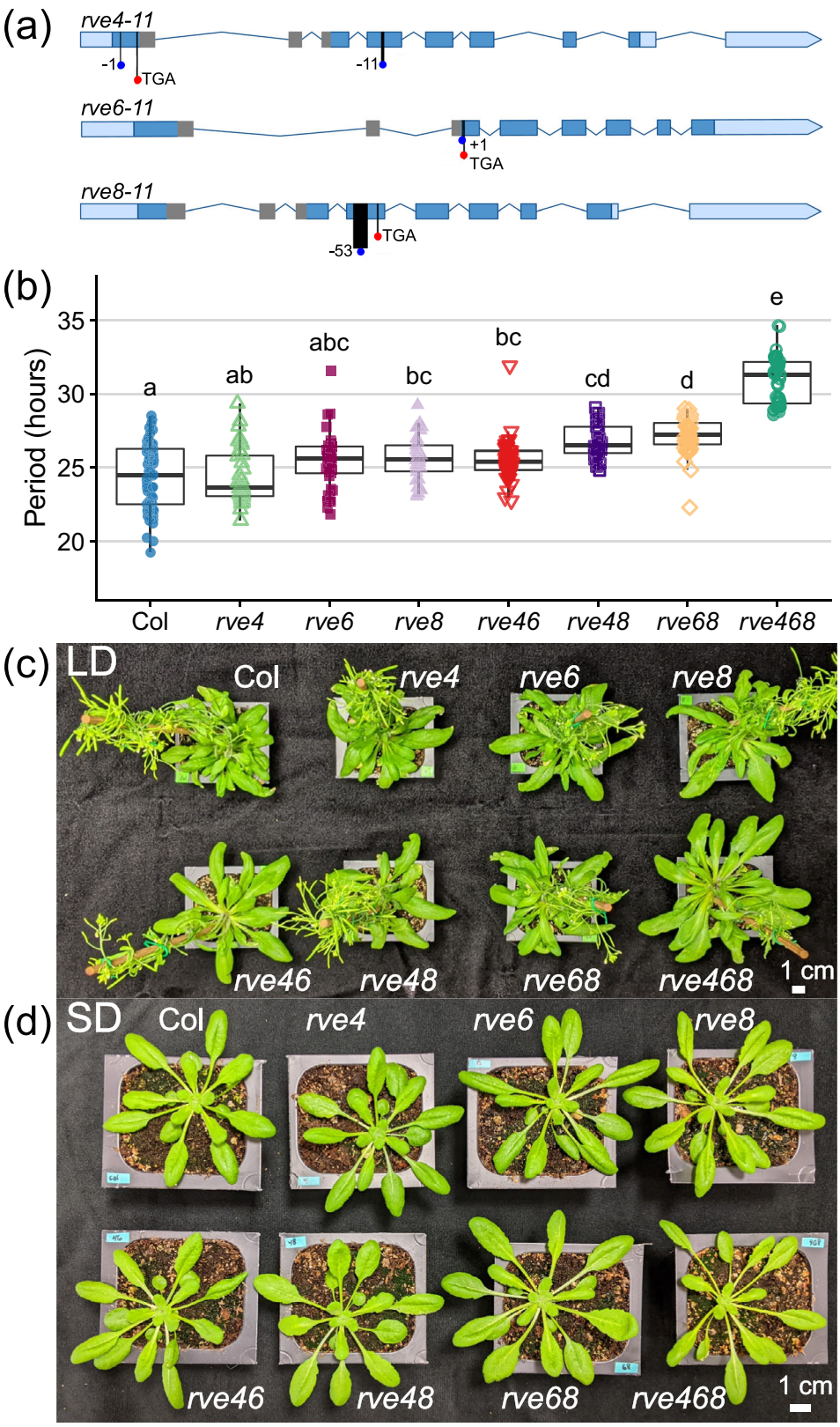

FIGURE 1 CRISPR-Cas9-generated *rve* mutants have phenotypes consistent with previously studied T-DNA *rve* mutants. (a) Gene models of *rve4-11*, *rve6-11*, and *rve8-11* alleles. Positions of insertions or deletions are shown by blue circles, and positions of resulting premature stop codons are shown by red circles. Light blue represents untranslated regions, while dark blue represents coding regions. Gray shading represents the coding regions of the Myb-like DNA-binding domains. (b) Period estimates of rhythmic seedlings (RAE < .6) for the indicated genotypes were determined by monitoring *CCR2::LUC2* expression. After entrainment, seedlings were transferred to constant 50 µmol m^{-2} s^{-1} red plus 50 µmol m^{-2} s^{-1} blue light. Different letters denote significant differences between genotypes ($p < 0.05$), determined by one-way ANOVA followed by Tukey's post hoc test. The lines within the boxes are the medians, and the lower and upper hinges represent the first and third quartiles. Data plotted are from three independent biological replicates ($n = 10–25$ per replicate). Representative images of plants grown for 35 days in (c) 16:8 light–dark cycles (long day [LD]) and (d) 8:16 light–dark cycles (short day [SD]).

RVE8 (Figure 1a). We then isolated all possible single and double mutant combinations and assessed growth and circadian clock phenotypes in these lines and the original triple mutant. These mutants will hereafter be referred to as *rve4*, *rve6*, *rve8*, *rve46*, *rve48*, *rve68*, and *rve468*. We first determined the free-running circadian period of seedlings by monitoring expression of a clock-regulated reporter gene, *CCR2::LUC2*, in each genotype. In constant red plus blue light, the *rve8* single, all three double, and the triple mutants have a significantly

longer period than Col-0 (Figure 1b). We also examined the growth of these *rve* mutants in long and short photoperiods (Figure 1c,d) and saw that *rve468* appears larger than Col-0 in long day conditions. These results are consistent with previous observations of *rve* triple mutants containing *rve4-1*, *rve6-1*, and *rve8-1* T-DNA alleles (Hsu et al., 2013).

An important trait governed by the circadian clock is the photoperiodic control of the transition from vegetative to reproductive growth (Maeda & Nakamichi, 2022; Song et al., 2015). It has previously been shown that *rve4-1 rve6-1 rve8-1* triple mutant plants flower significantly later than Col-0 in long day photoperiods (Gray et al., 2017), so we hypothesized that other long-period *rve* mutants would also flower late. However, only *rve46*, *rve68*, and *rve468* flower significantly later than Col-0 in long days when measured by leaf number at flowering (Figure S1A). The *rve4*, *rve6*, *rve8*, and *rve48* mutants do not flower later than Col-0 (Figures 2a and S1A), even though *rve8* and *rve48* have long circadian periods quite similar to those of *rve46* and *rve68*, respectively (Figure 1b). In short day photoperiods, none of the *rve* mutants have a significantly different flowering time from Col-0 when measured by leaf number at flowering (Figures 2a and S1A), although *rve468* flowers significantly later when measured by days to flowering (Figure 2b). Overall, the delayed flowering time of *rve468* triple mutants compared with the single and double mutants in long days suggests that *RVE4*, *RVE6, and RVE8* act synergistically but not equally in regulation of flowering time.

We continued to examine the phenotypes of adult *rve* mutants in long and short photoperiods by measuring the petiole length and blade area of the fully expanded fifth rosette leaf. In long and short days, the median petiole length of the *rve* single mutants is not significantly different from that of Col-0, but *rve68* and *rve468* have significantly longer petioles in short days (Figures 2c and S1C). The median blade area of all *rve* mutants trends larger than Col-0 in long days, although this only reaches statistical significance for *rve468* (Figures 2d and S1D). This is consistent with our previous findings that *rve468* T-DNA mutants have larger leaf blades than Col-0 when grown in long days (Gray et al., 2017). Surprisingly, in short days, the median blade area of *rve* mutants trends smaller than Col-0, although again, this is only statistically significant for *rve468* (Figures 2d and S1D). Although there are not many significant differences in leaf growth between the *rve* mutants and Col-0, together, these data suggest that these three RVE proteins act redundantly in control of leaf growth and that their roles differ depending on day length.

We next investigated the roles for RVE proteins in photomorphogenesis. Seedlings were grown in constant darkness or in a range of fluence rates of constant monochromatic red, monochromatic blue, or red plus blue light, and hypocotyl lengths were measured. In constant darkness, all *rve* mutants except *rve48* have significantly longer hypocotyls than Col-0 (Figures 3 and S2), suggesting a role in light-independent regulation of development. To test whether the RVEs also function in photoreceptor signaling pathways, we assessed inhibition of hypocotyl elongation at a range of fluence rates of red, blue, and red plus blue light (Figures 3 and S2). The responsiveness of the *rve468* triple mutant is significantly different from wild type in red and in red plus blue light in this assay (Table S1). This suggests that these transcription factors have both light-dependent and red light-specific roles in growth regulation.

We next examined hypocotyl elongation phenotypes in the single and double mutants. In all three light qualities tested, all *rve* single mutants have significantly longer hypocotyls than wild type at one or more light intensities (Figure S2), with loss of *RVE6* giving the strongest phenotype. Intriguingly, hypocotyl elongation in *rve48* double mutants is not significantly different from wild type in the dark or at lower light intensities, despite the significantly long hypocotyls of both *rve4* and *rve8* single mutants in these conditions (Figure 3). These data suggest a light-independent, antagonistic relationship between RVE4 and RVE8 in the control of hypocotyl elongation.

The stronger hypocotyl phenotypes seen for *rve6* than for *rve4* and *rve8* suggest that *RVE6* is more important than these other Myb-like factors in the regulation of photomorphogenesis. Indeed, the slope of *rve6*, but not the other single mutants, is significantly different from wild type in monochromatic blue light and in red plus blue light (Table S1). Also consistent with a major role for *RVE6*, while the *rve46* and *rve68* double mutants both have significantly elongated hypocotyls at most fluence rates in all three conditions, the *rve68* phenotypes are generally quite similar to the long hypocotyl phenotypes of the triple *rve468* mutant seedlings (Figure S2). Together, these data suggest that all three *RVE* genes contribute to regulation of photomorphogenesis in response to both red and blue light but that RVE6 plays a predominant role.

2.2 | *rve468* mutants follow Aschoff's rule in monochromatic red but not monochromatic blue light

We next examined the circadian phenotypes of the *rve* single, double, and triple mutants in a variety of light conditions (constant darkness, monochromatic red, monochromatic blue, and constant red plus blue light) and across a range of light intensities (from 1 to 200 μmol m^{-2} s^{-1}). We previously reported that the T-DNA alleles of *rve4* and *rve6* did not have period phenotypes (Hsu et al., 2013). While the new CRISPR allele of *rve4* does not have a period significantly different from wild type in any of the conditions tested, the new *rve6* allele has a significantly long-period phenotype in red light, and both *rve6* and *rve8* single mutants trend long period in red plus blue but not monochromatic blue light (Figure 4). This suggests RVE6 and RVE8 play more important roles in clock function than RVE4. Indeed, while all three double mutant combinations have long-period phenotypes, the *rve68* mutant has a consistently longer period than the other two double mutants (Figure S3). However, because free-running period is the longest in the triple *rve468* mutant (Figure S3), all three *RVE* genes contribute to period shortening in all light conditions tested.

We previously noted that increasing intensities of monochromatic red and monochromatic blue light have opposite effects on *rve4-1 rve6-1 rve8-1* period (Gray et al., 2017). We therefore wanted to determine if other *rve* mutants have similar differences in circadian

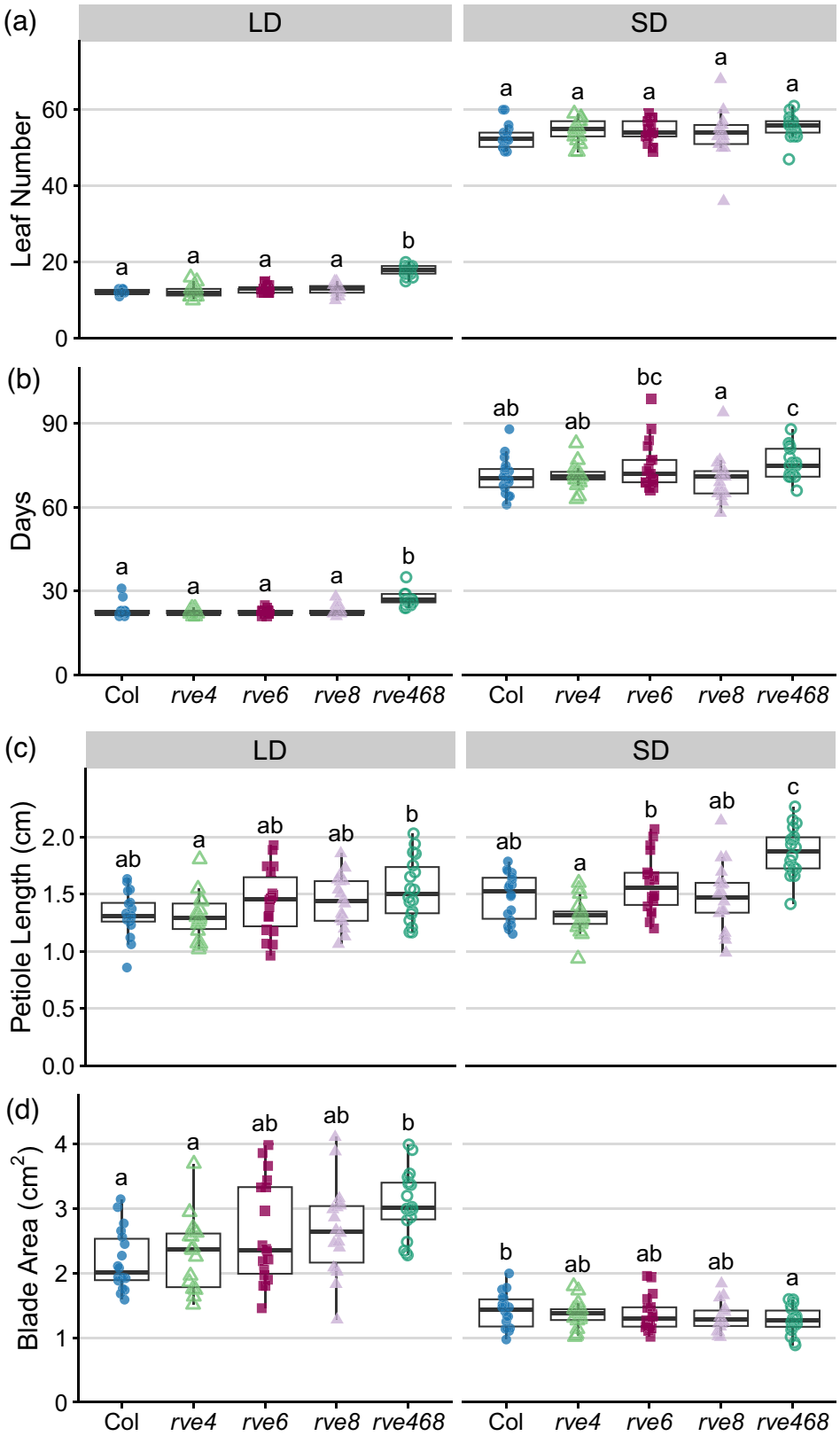

FIGURE 2 RVEs act redundantly to control flowering time and leaf growth. Flowering time of the indicated genotypes was assessed by leaf number at bolting (a) and days to bolting (b). $n = 17–18$, experiment was conducted twice with similar results. Petiole length (c) and blade area (d) of rosette leaf 5 of the indicated genotypes were assessed after 30 days of growth in the specified photoperiods. $n = 18$, experiment was conducted twice with similar results. (a–d) Plants were grown under 150–200 µmol m^{-2} s^{-1} white light in the specified photoperiods (16:8 long day [LD] or 8:16 short day [SD]). Different letters denote significant differences between genotypes within each condition ($p < 0.05$), determined by one-way ANOVA followed by Tukey's post hoc test. The lines within the boxes are the medians, and the lower and upper hinges represent the first and third quartiles.

responsiveness to light. To investigate this, we assessed the slopes of free-running period relative to fluence rate in red, blue, and red plus blue light. In red light, the period of all single, double, and triple *rve* mutants decreases as light intensity increases (Figures 4 and S3), with slopes not significantly different from Col-0 (two-way ANOVA and Tukey's post hoc test, $p > 0.05$; Table S1). Thus, in red light, the *rve* mutants and wild type show similar sensitivity to light input to the clock and obey Aschoff's (1979) rule for diurnal organisms.

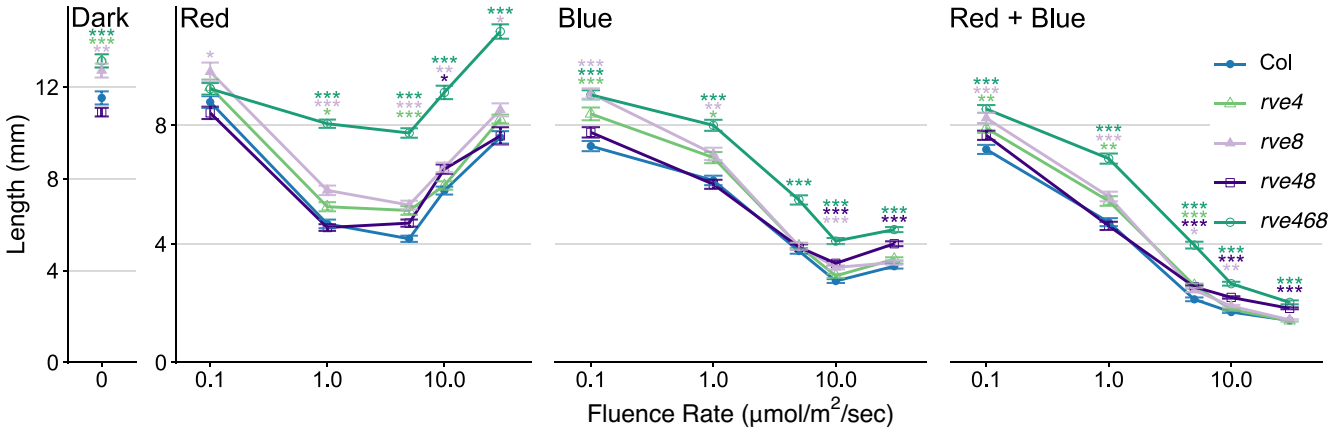

FIGURE 3 RVE4 and RVE8 have epistatic effects on hypocotyl elongation. Hypocotyl lengths of the indicated genotypes were determined in constant darkness or monochromatic red, monochromatic blue, or red plus blue light of the specified intensities (0.1–30 µmol m^{-2} s^{-1}). Points indicate mean hypocotyl lengths; error bars indicate ±SEM. Significant differences between genotypes determined by one-way ANOVA followed by Tukey's post hoc test (*p < 0.05, **p < 0.01, ***p < 0.001). Data plotted are from three (light conditions) or six (constant darkness) biological replicates (n = 7–24 per replicate).

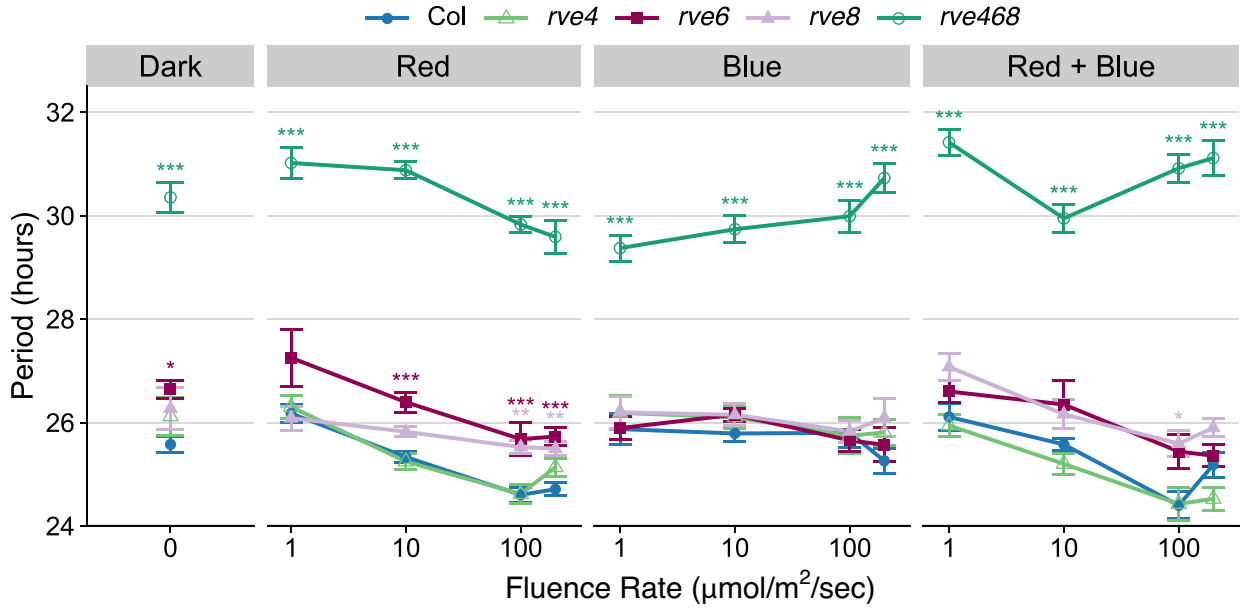

FIGURE 4 Increasing intensities of blue and red light have opposite effects on circadian period in *rve468* mutants. Period estimates of rhythmic seedlings (RAE < .6) for the indicated genotypes were determined in constant darkness or constant monochromatic red, monochromatic blue, or red plus blue light of the specified intensities (1–200 µmol m^{-2} s^{-1}) by monitoring *CCR2::LUC2* expression. Points indicate mean periods; error bars indicate ±SEM. Significant differences between genotypes determined by one-way ANOVA followed by Tukey's post hoc test (*p < 0.05, **p < 0.01, ***p < 0.001). Data plotted are from three independent biological replicates (n = 6–81 per replicate).

It has previously been reported that in Arabidopsis, circadian period is less responsive to changes in blue light intensity compared with red light intensity (Covington et al., 2001). This may be related to the fact that both the cryptochrome and ZTL families of photoreceptors mediate blue light signaling whereas phytochromes are the primary mediators of red light signaling to the circadian system (Sanchez et al., 2020). Consistent with relative insensitivity of the Arabidopsis circadian system to blue light intensity, we observed little change in period for wild type, the *rve* single mutants, and the *rve46* and *rve68* double mutants over the fluence rates of blue light tested (Table S1). In contrast, the period of *rve468* and *rve48* increases as light intensity increases with slopes that are not significantly different from each other but that are significantly different from wild type (Figure S3 and Table S1). This pattern of period lengthening at higher light intensities is reminiscent of responses seen in many nocturnal organisms. This difference in response of circadian period to red and blue light in *rve468* and *rve48* mutants suggests that *RVE4* and *RVE8* regulation or function is altered between these two light qualities.

2.3 | Blue light-mediated enhancement of expression of some clock genes is lost in *rve468* mutants

Given the different effects of red and blue light on circadian period in *rve468* mutants, we hypothesized that expression of clock genes might be altered in *rve468* in a light quality-specific manner. To assess this, we grew Col-0 and *rve468* seedlings in monochromatic blue or monochromatic red light, collected samples over a 24 h period, extracted RNA, and carried out quantitative reverse-transcriptase polymerase chain reaction (qRT-PCR) assays. In wild-type plants, the amplitude of the evening-phased clock gene *ELF4* is significantly higher in blue than in red light (Figures 5 and S4A). A similar trend is seen for the other evening-phased genes *TOC1* and *PRR5*, although the differences in these values do not reach statistical significance (Figure S4). In the case of *PRR5*, this may be because its expression pattern in blue light poorly matches a cosine curve, leading to an underestimate of its amplitude. A previous study found a significant increase in peak levels of *PRR5* expression in blue light compared with red (Hajdu et al., 2018), suggesting that its levels are indeed induced by blue light. However, we found that blue light did not cause a significant increase in peak levels of *CCA1*, *LUX*, and *BOA* when compared with red light treatments (Figures 5 and S4A). These data show that blue light enhances expression of a subset of evening-phased clock genes in wild type.

We next compared expression patterns of these genes in *rve468* mutants maintained in constant red or blue light. Unlike in wild type, blue light does not cause an increase in amplitude of *ELF4*, *TOC1*, or *PRR5* expression in *rve468* (Figures 5 and S4A). We observed similar patterns when this experiment was conducted using the *rve4-1 rve6-1 rve8-1* T-DNA mutant (Figures S4B and S5). These data show that RVE function is required for the blue-light mediated enhancement of expression of a subset of clock genes, which may help explain the stronger period phenotype observed in *rve468* maintained in high-intensity blue compared with high-intensity red light (Figure 4). Intriguingly, *ELF4*, *TOC1*, and *PRR5* are all direct targets of RVE8 transactivation activity (Hsu et al., 2013).

2.4 | Blue-specific *rve* mutant phenotypes are not due to differences in RVE protein abundance or degradation rate

We hypothesized that the blue light-specific phenotypes observed in *rve* mutants might be due to higher *RVE* transcript levels in this condition. However, we did not observe any differences in *RVE4*, *RVE6*, or *RVE8* transcript abundance in plants maintained in constant red or blue light (Figure S6). We next assessed protein levels in the two conditions, making use of plants expressing epitope-tagged RVE4 or RVE8 under control of their native promoters. We focused on these

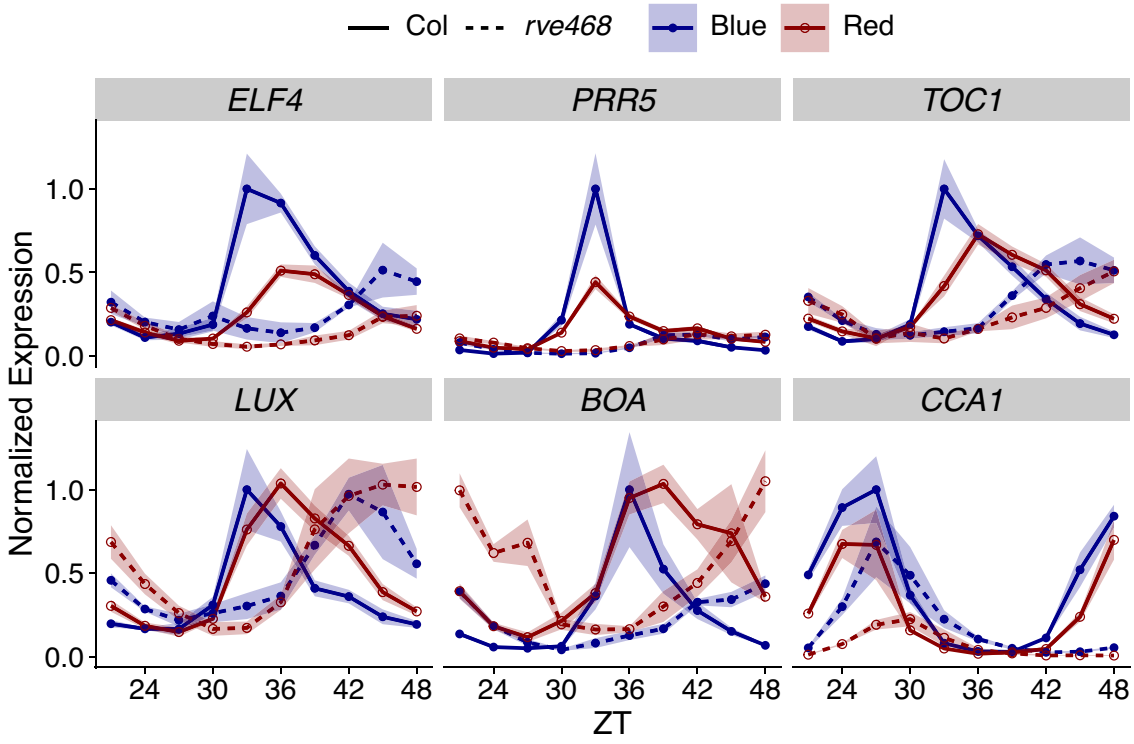

FIGURE 5 Blue-mediated enhancement of clock gene expression is reduced in *rve468* mutants. After entrainment, Col-0 and *rve4-11 rve6-11 rve8-11* seedlings were transferred at ZT0 to constant 60 μmol m^{-2} s^{-1} monochromatic blue or monochromatic red light. Expression of the specified genes was determined by qRT-PCR and normalized to reference genes *PP2A* and *IPP2*. Ribbon indicates ±SEM for three biological replicates.

two proteins because of the blue light-specific period responses in *rve48* and *rve468* mutants (Figure S3). The *RVE8::RVE8-HA* transgene has previously been reported to rescue *rve8-1* phenotypes (Rawat et al., 2011), and we similarly found that *RVE4::RVE4-FLAG* rescues RVE4 function in the *rve4-1* and *rve4-1 rve8-1* mutant backgrounds (Figure S7). Seedlings were grown in various light conditions (monochromatic blue, monochromatic red, constant white light, 12:12 light–dark cycles, or constant darkness), samples were collected at 4 h intervals, and proteins were extracted and detected by western blotting. We found that the pattern of both RVE4-FLAG and RVE8-HA abundance is similar across light conditions (Figure 6a) but that abundance of both proteins decreases rapidly in constant darkness (Figures 6a and S8). However, RVE4-FLAG and RVE8-HA abundance is similar between monochromatic blue and monochromatic red light (Figures 6a and S8), indicating that the stronger *rve* phenotypes in blue light compared with red are not due to a difference in RVE protein levels.

For many activators of transcription, activity is tightly coupled to their proteasome-mediated degradation (Geng & Tansey, 2012;

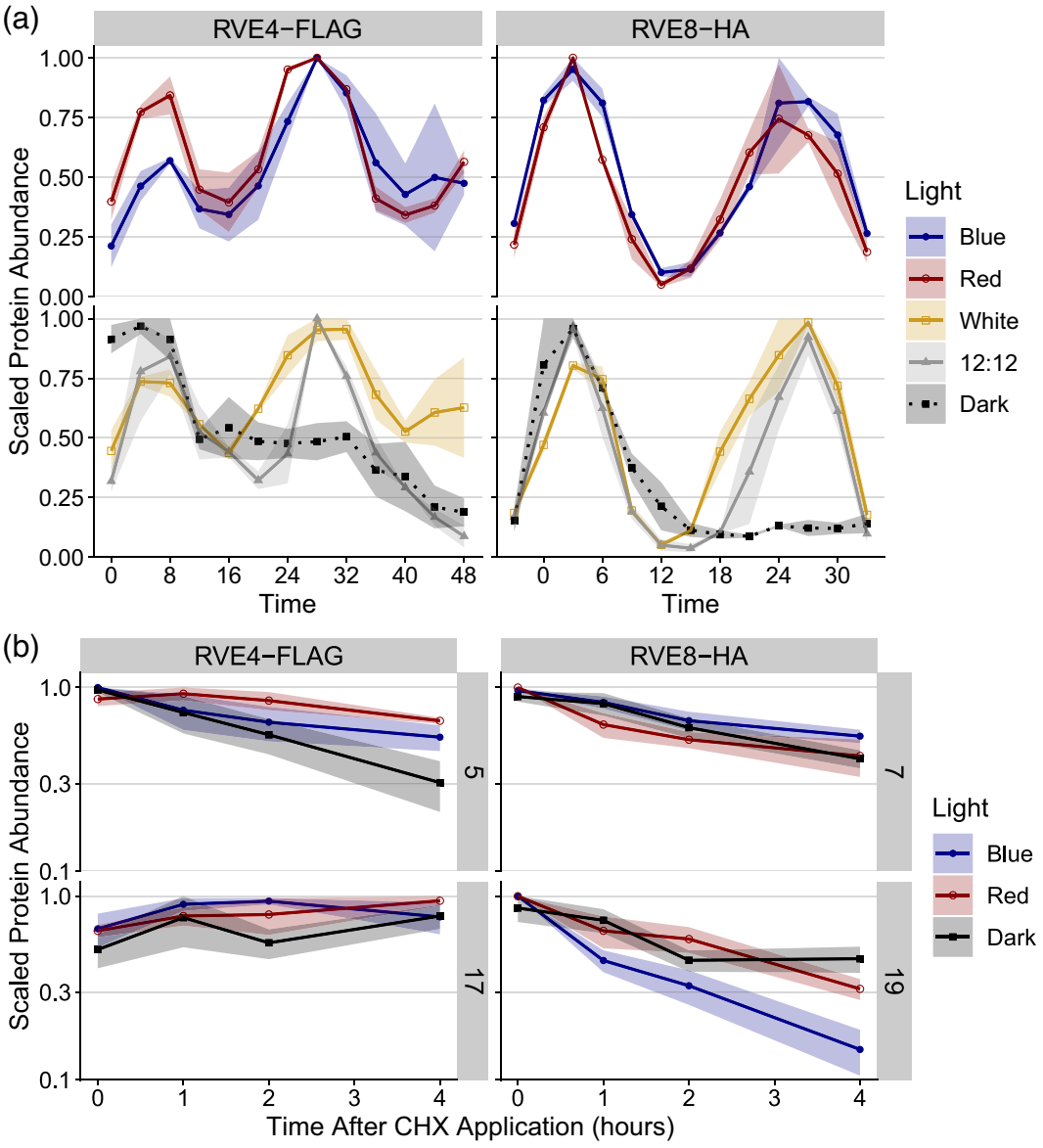

FIGURE 6 RVE4-FLAG and RVE8-HA protein abundance and degradation rates are similar in monochromatic red and monochromatic blue light. (a) After entrainment, seedlings were kept in 12:12 light–dark cycles under 50–60 μmol m^{-2} s^{-1} white light or transferred at Time 0 to constant darkness, constant 50–60 μmol m^{-2} s^{-1} white, 60 μmol m^{-2} s^{-1} monochromatic blue, or 60 μmol m^{-2} s^{-1} monochromatic red light. Abundance of the specified proteins was determined by western blot and normalized to abundance of actin. Ribbon indicates ±SEM for two biological replicates. (b) After entrainment, seedlings were transferred at ZT0 to constant darkness, 60 μmol m^{-2} s^{-1} monochromatic blue, or 60 μmol m^{-2} s^{-1} monochromatic red light. Seedlings were treated with cycloheximide (CHX) during the day (at ZT5 or ZT7) or during the subjective night (at ZT17 or ZT19). Abundance of the specified proteins was determined by western blot and normalized to abundance of actin. For RVE4-FLAG, ribbon indicates ±SEM for three biological replicates. For RVE8-HA, ribbon indicates ±SEM for seven biological replicates in blue, four biological replicates in red, and five biological replicates in the dark.

Lipford & Deshaies, 2003; Muratani & Tansey, 2003; Zhai et al., 2013). Because RVE8 is a direct transcriptional activator of genes such as *PRR5*, *ELF4*, and *TOC1* (Hsu et al., 2013), which have enhanced peak levels in blue light compared with red (Figures 5 and S5), we speculated that higher RVE activity in blue light might be accompanied by an increase in RVE protein degradation in this condition. To test this, we exposed seedlings expressing RVE4-FLAG or RVE8-HA to various light conditions (monochromatic blue, monochromatic red light, or constant darkness), applied cycloheximide during the day or subjective night to inhibit translation of new proteins, and assessed RVE protein abundance over time by western blotting. RVE4-FLAG is relatively stable during both the day (ZT5) and subjective night (ZT17), and its degradation rate is not significantly different in plants maintained in monochromatic blue or red light at either time (Figure 6b; exponential decay model, Bayesian posterior probability of equal degradation rates in red and blue: .90 and .96 for ZT5 and ZT17, respectively). For RVE8-HA, there is no significant difference in RVE8-HA protein degradation rate between monochromatic blue and monochromatic red light during the day (Figure 6b; exponential decay model, Bayesian posterior probability of equal degradation rates in red and blue: .93 at ZT7). Surprisingly, however, RVE8-HA is degraded more quickly in blue than in red during the subjective night (Figure 6b; exponential decay model, Bayesian posterior probability of degradation rate in blue > red = 1). But given that RVE8 is active around midday and not during the night (Hsu et al., 2013), these data suggest that the observed differences in *rve* circadian phenotypes in plants maintained in red and blue light (Figures 4 and 5) are not due to a difference in RVE4 or RVE8 protein degradation rates in these conditions.

2.5 | Blue-specific *rve* mutant phenotypes do not require *ZTL* or *HY5*

We next hypothesized that the *rve468* blue-light specific phenotypes might be caused by interactions between the *RVEs* and a blue light-specific factor. Two such factors known to influence the circadian system are the blue light photoreceptor ZTL and the blue light-stabilized transcription factor HY5. We first tested for a genetic interaction between *RVE8* and *ZTL* by assessing free-running circadian period in *rve8-1 ztl-103* double mutants and *rve8-1* and *ztl-103* single mutants in a range of fluence rates of monochromatic blue light. Both *rve8-1* and *ztl-103* have long-period phenotypes, and the period of *rve8-1-ztl-103* is additively longer than the single mutants (Figure S9A). We also examined the stability of RVE8-HA protein in a *ztl* mutant background and found no significant difference in protein degradation rates between monochromatic blue and monochromatic red light during the subjective night (Figure S9B, exponential decay model, Bayesian posterior probability of rates being equal: .79). Bayesian analysis reveals that during the day, the RVE8-HA protein degradation rate is slower in *ztl* mutants in blue light than in red light (posterior probability for rate in red > rate in blue = 1). Finally, the degradation rates of RVE8-HA in blue light are similar in wild type and in *ztl* mutants in both the subjective day and night (Figure S9B, exponential decay model, Bayesian posterior probability for equivalent rates in *ztl* and wild type = .96 at ZT7 and .95 at ZT19). This, along with the additive effects of the *rve8* and *ztl* mutations on circadian period (Figure S9A), suggests that the ZTL and RVE8 proteins affect the circadian system via different mechanisms. Overall, these data suggest that an interaction between *RVE8* and *ZTL* is not responsible for the blue light-specific phenotypes of *rve* mutants.

We next tested for a genetic interaction between *RVE4*, *RVE6*, *RVE8*, and *HY5* by examining the circadian and growth phenotypes of *rve468 hy5* mutants compared with *rve468* and *hy5*. In constant red light, *hy5* single mutants do not have a period phenotype and *rve468 hy5* and *rve468* mutants do not have a difference in free-running period (Figure 7a). However, in constant monochromatic blue light of moderate intensity, *hy5* has a significantly shorter period and *rve468* has a significantly longer period than Col-0 (Figure 7a), consistent with previous observations (Gray et al., 2017; Hajdu et al., 2018).

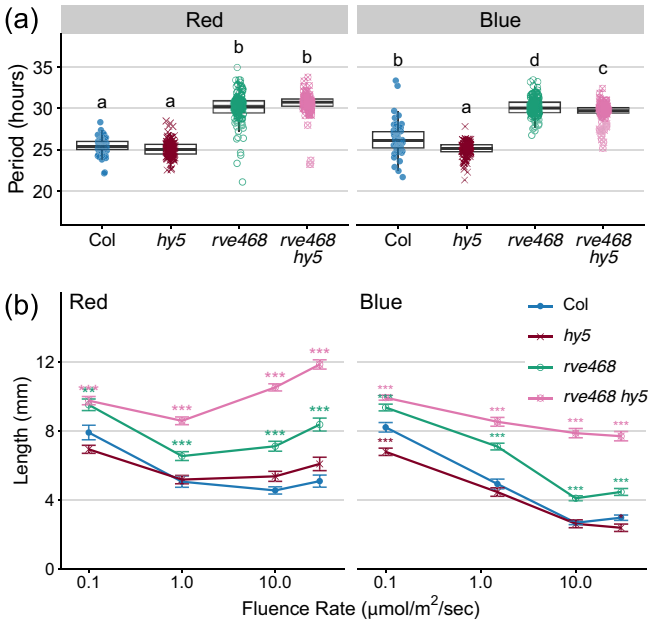

FIGURE 7 *RVE4*, *RVE6*, *RVE8*, and *HY5* interact additively to control clock function but epistatically to control hypocotyl elongation. (a) Period estimates of rhythmic seedlings (RAE < .6) for the indicated genotypes were determined by monitoring *CCR2::LUC2* expression. After entrainment, seedlings were transferred to constant 15 µmol m^{-2} s^{-1} monochromatic red or blue light. Different letters denote significant differences between genotypes ($p < 0.01$), determined by one-way ANOVA followed by Tukey's post hoc test. The lines within the boxes are the medians, and the lower and upper hinges represent the first and third quartiles. Data plotted are from two independent biological replicates ($n = 42–77$ per replicate). (b) Hypocotyl lengths of the indicated genotypes were determined in constant monochromatic red or blue light of the specified intensities (0.1–30 µmol m^{-2} s^{-1}). Points indicate mean hypocotyl length; error bars indicate ±SEM. Significant differences between genotypes determined by one-way ANOVA followed by Tukey's post hoc test (*$p < 0.05$, **$p < 0.01$, ***$p < 0.001$). Data plotted are from two biological replicates ($n = 16–24$ per replicate).

Interestingly, *rve468 hy5* has a significantly longer period than Col-0 but a significantly shorter period than *rve468* (Figure 7a), which suggests that the *RVEs* and *HY5* interact additively to regulate circadian period in monochromatic blue light. Similar to our findings for *RVE8* and *ZTL*, the additive interaction between *RVE4*, *RVE6*, *RVE8*, and *HY5* in this assay suggests that an interaction between the *RVEs* and *HY5* is not responsible for the observed blue light-specific circadian phenotype of *rve* mutants.

We next assessed light-mediated inhibition of hypocotyl elongation in these mutants. We found that *rve468 hy5* hypocotyls are considerably longer than *rve468* hypocotyls in both red and blue light at almost all light intensities tested (Figure 7b). Moreover, in both colors of light, the *rve468 hy5* fluence–response slope is significantly different than that of Col-0 and *rve468* (Table S1). In red light, the responsiveness of *rve468 hy5* is also different from that of the *hy5* single mutant. These data indicate that these quadruple mutant seedlings have altered sensitivity to light when compared with both the wild type and the parental *rve468* and *hy5* mutants. Thus, in contrast to their blue-specific and additive effects on clock function, HY5 and the RVEs play synergistic roles in the regulation of hypocotyl elongation in both blue and red light.

3 | DISCUSSION

Here, we present new mutant alleles of *RVE4*, *RVE6*, and *RVE8* in various combinations and show that they have similar clock and growth phenotypes to the previously studied T-DNA alleles (Gray et al., 2017; Hsu et al., 2013). However, we find that the *rve6* truncation mutant has a circadian clock phenotype not seen for the *rve6* T-DNA allele and that the new, likely null, *rve468* mutant characterized here has a stronger circadian phenotype than the *rve4-1 rve6-1 rve8-1* T-DNA line we originally characterized (Hsu et al., 2013). These results are likely because the original *rve6-1* allele reduced rather than abolished *RVE6* expression. We believe that the single, double, and triple mutant CRISPR-Cas9-generated alleles we have generated will be extremely useful in future studies, especially given that after generations of propagation, the original *rve4-1 rve6-1 rve8-1* mutants have also regained moderate expression of *RVE4* and *RVE8* (Hughes & Harmer, 2023).

3.1 | Severity of *rve* growth and clock phenotypes depends on light quality and intensity

Our detailed characterization of *rve* single, double, and triple mutants has allowed us to assess their relative importance for regulation of plant growth and the circadian clock (Figure S10). When examining phenotypes in monochromatic red and monochromatic blue light, we found it surprising that the severity of growth and clock phenotypes does not always match based on the light conditions. For example, all *rve* single mutants have a long-hypocotyl phenotype in lower levels of monochromatic blue light, particularly at .1 μmol m^{-2} s^{-1} (Figure S2), but none of these mutants have a period phenotype in any of the tested fluence rates of blue light (Figure 4). Similarly, all *rve* single mutants have significantly long hypocotyls in constant darkness (Figure S2), but only *rve6* has a significantly long period in constant darkness (Figure 4). With the double mutants, *rve46* has significantly long hypocotyls in .1 and 1 μmol m^{-2} s^{-1} monochromatic blue light (Figure S2) but no period phenotype in those same light conditions (Figure S3). These phenotypic differences suggest that the RVE proteins have separate functions in regulation of growth and the clock.

We also noted differences in the effects of loss of the *RVEs* on the sensitivity of photomorphogenesis and the circadian system to light. As noted above, the circadian period of both *rve48* and *rve468* increases with higher fluence rates of monochromatic blue light while that of wild type does not significantly change (Figures 4 and S3 and Table S1). In contrast, in hypocotyl fluence rate response curves, *rve468* displays an altered sensitivity to red but not blue light when compared with wild type (Figures 3 and S2 and Table S1). These results suggest that in addition to playing separable roles in control of photomorphogenesis and circadian clock function, *RVE4*, *RVE6*, and *RVE8* are also separately involved in different photoreceptor signaling pathways to the clock.

3.2 | Possible mechanisms underlying light quality-dependent regulation of *RVE* function

Our initial hypothesis that the enhanced circadian period phenotype of *rve48* and *rve468* mutants in response to blue light (Figure S3) might be due to increased RVE4 or RVE8 protein abundance in this condition proved incorrect (Figures 6 and S8). However, there may be a light quality-specific difference in *RVE* transcript instead of RVE protein. While the overall abundance of *RVE4*, *RVE6*, and *RVE8* transcript in Col-0 is similar in monochromatic blue and monochromatic red light (Figure S6), alternative splicing of these transcripts could differ between light qualities. Alternative splicing of *RVE8* has been observed to be regulated in response to white light (Mancini et al., 2016), and increased abundance of a particular *RVE8* isoform has been associated with increased amplitude of *RVE8* target gene expression (Yan et al., 2022). Perhaps alternative splicing generating an isoform with distinct activity is increased in monochromatic blue light compared with monochromatic red light, leading to the observed amplitude difference in some evening-phased clock genes between these two light conditions (Figure 5).

Another possibility is that the localization of RVE proteins could differ in blue and in red light. The nuclear localization of both RVE4 and RVE8 has been shown to increase in seedlings moved from 22°C to 4°C and subsequently decrease when the seedlings were moved back to 22°C (Kidokoro et al., 2021). RVE proteins might be primarily localized in the nucleus when exposed to monochromatic blue light but primarily localized in the cytoplasm under monochromatic red light. Increased nuclear localization in blue light conditions would allow for increased activation of *RVE* targets, which could account for the enhanced expression of RVE8 target genes in blue compared with red light seen in wild type but not in *rve468* (Figure 5).

Finally, another possibility is that RVE4 and RVE8 interact with a blue-light specific signaling component that helps control clock period.

Our genetic analysis suggests that the RVEs are not specifically working with ZTL or HY5 in control of clock pace in blue light (Figures S9 and 7). However, a recent report has revealed roles for the clock protein PRR9 and the blue light photoreceptor CRY2 in circadian clock sensitivity to blue light (He et al., 2022). It is possible that the RVEs act with these or other, yet unidentified factors, in the transduction of blue light signals to the circadian system.

4 | MATERIALS AND METHODS

4.1 | Plant materials

All plants used are in the Columbia (Col-0) wild-type background. Col *CCR2::LUC2* and *rve4-11 rve6-11 rve8-11 CCR2::LUC2* were generated as previously described (Hughes & Harmer, 2023). The *rve4-11 rve6-11 rve8-11 CCR2::LUC2* mutant was then backcrossed to Col *CCR2::LUC2* to generate *rve4-11 CCR2::LUC2*, *rve6-11 CCR2::LUC2*, *rve8-11 CCR2::LUC2*, *rve4-11 rve6-11 CCR2::LUC2*, *rve4-11 rve8-11 CCR2::LUC2*, and *rve6-11 rve8-11 CCR2::LUC2* mutants. *RVE4::RVE4-FLAG rve4-1 CCR2::LUC+* and *RVE4::RVE4-FLAG rve4-1 rve8-1 CCR2::LUC+* were generated by transforming *rve4-1 CCR2::LUC+* and *rve4-1 rve8-1 CCR2::LUC+*, respectively, with *RVE4::RVE4-FLAG* via floral dip (Clough & Bent, 1998). *RVE8::RVE8-HA rve8-1* was previously described (Rawat et al., 2011). Col *CCR2::LUC2* was crossed to *hy5* (SALK_096651) (Chen et al., 2008) to generate *hy5 CCR2::LUC2*. *rve4-11 rve6-11 rve8-11 hy5 CCR2::LUC+* was crossed to *rve4-11 rve6-11 rve8-11 CCR2::LUC2* to generate *rve4-11 rve6-11 rve8-11 hy5 CCR2::LUC2*. For Figure S4, Col *CCR2::LUC+* and *rve4-1 rve6-1 rve8-1 CCR2::LUC+* are as previously described (Hsu et al., 2013; Rawat et al., 2011). For Figure S9, Col *CCR2::LUC+*, *rve8-1 CCR2::LUC+*, and *ztl-103 CCR2::LUC+* are as previously described (Martin-Tryon et al., 2007; Rawat et al., 2011). The *rve8-1 ztl-103 CCR2::LUC+* mutant was generated by crossing *rve8-1 CCR2::LUC+* to *ztl-103 CCR2::LUC+*. *RVE8::RVE8-HA rve8-1 ztl-103* was generated by crossing *RVE8::RVE8-HA rve8-1* to *ztl-103 CCR2::LUC+*.

4.2 | Plasmids

RVE4::RVE4-FLAG was created by first amplifying the *RVE4* genomic region using primers 5′-CGGCAAGTATCTCCATTAGAT-3′ and 5′-AGAGCTTAAGTGTTCATGACC-3′. The amplified region, including approximately 2 kb upstream of the transcriptional start site, was cloned into pCR8 (Invitrogen, Carlsbad, CA), which was then recombined with pEarleyGate302 by Gateway cloning (Hartley et al., 2000).

4.3 | Genotyping

CRISPR-Cas9 alleles were identified through PCR amplification followed by Sanger sequencing, as previously described (Hughes & Harmer, 2023). Mutant lines without Cas9 were selected for use in experiments. Homozygous mutants of all alleles used in this research were identified through PCR amplification of genomic DNA. Primers used for genotyping are included in Table S2.

4.4 | Growth conditions

Seeds were surface sterilized with chlorine gas and stratified in the dark for 2–4 days at 4°C. For luciferase imaging, qRT-PCR, and western blotting, seeds were plated on 1X Murashige and Skoog, .7% agar, and 3% sucrose. Seedlings were entrained in light–dark cycles (12 h light, 12 h dark) under 50–60 μmol m^{-2} s^{-1} white light at 22°C for 6 days. For hypocotyl length assays, seeds were plated on .5X Murashige and Skoog and .7% agar and exposed to a 4 h pulse of 50–60 μmol m^{-2} s^{-1} white light at 22°C to induce germination. Seedlings were then grown in the specified light conditions using monochromatic red and/or blue LEDs (XtremeLUX, Santa Clara, CA) at 22°C for 6 days. For flowering time and rosette growth assays, seeds were sown directly on soil and grown in light–dark cycles of the specified photoperiod under 150–200 μmol m^{-2} s^{-1} white light at 22°C.

4.5 | *CCR2::LUC2* and *CCR2::LUC+* luciferase imaging

Seedlings were sprayed with 3 mM D-luciferin, moved to the specified light conditions using red and/or blue LEDs (XtremeLUX, Santa Clara, CA), and imaged for 5–6 days under a cooled CCD camera (DU434-BV, Andor Technology, or iKon M-934, Andor Technology, or ORCA II ER CCD, Hamamatsu Photonics). Neutral density filters (Rosco Laboratories or LEE Filters) were used to generate the specified light intensities of monochromatic red, monochromatic blue, or red plus blue light (Figures 4 and S3). Quantification of bioluminescence was performed using MetaMorph software (Molecular Devices), and circadian rhythms were analyzed with Biological Rhythm Analysis Software System (Locke et al., 2005).

4.6 | qRT-PCR analysis

After entrainment, seedlings were exposed to constant 60 μmol m^{-2} s^{-1} monochromatic blue or red light under LEDs (XtremeLUX, Santa Clara, CA) at 22°C. Seedlings were moved at dawn (ZT0) and collected every 3 h from ZT21 to ZT48 (Figures 5 and S6) or every 3 h from ZT24 to ZT48 (Figure S4). Sample preparation and qRT-PCR were performed as previously described (Shalit-Kaneh et al., 2018) using a BioRad CFX96 thermocycler (Bio-Rad Laboratories, Hercules, CA). Relative expression and SEM values were obtained from the BioRad CFX96 software package, and amplitudes were calculated using BioDare2 (Zielinski et al., 2014). Primers used for qRT-PCR are included in Table S2.

4.7 | Hypocotyl length assays

After 6 days of growth, seedlings were transferred to transparent sheets and scanned at 600 dpi. Hypocotyls were individually measured using ImageJ (Schneider et al., 2012).

4.8 | Flowering time analysis

Date of flowering was recorded as the day the inflorescence stem reached 1 cm long. At that time, rosette leaves were counted to determine flowering time by leaf number. Cauline leaves were not included.

4.9 | Rosette leaf measurements

After 30 days of growth, rosette leaf 5 was transferred to transparent sheets and scanned at 600 dpi. Blade area and petiole length were measured using LeafJ (Maloof et al., 2013).

4.10 | Protein abundance assays

After entrainment, seedlings were exposed to constant darkness, constant 60 μmol m^{-2} s^{-1} monochromatic blue or red light under LEDs (XtremeLUX, Santa Clara, CA), or 50–60 μmol m^{-2} s^{-1} white light at 22°C. Seedlings were moved at dawn (Time 0) and collected every 4 h from Times 0 to 48 (RVE4-FLAG) or every 3 h from 3 h before dawn to Time 33 (RVE8-HA). Samples were prepared and quantified as previously described (Shalit-Kaneh et al., 2018). Total protein was analyzed by western blotting using mouse monoclonal anti-FLAG M2-HRP antibody (Sigma-Aldrich, St. Louis, MO) for RVE4-FLAG and rat monoclonal anti-HA-HRP antibody (Roche, Basel, Switzerland) for RVE8-HA. Prometheus ProSignal Dura (Genesee Scientific, Rochester, NY) was used to generate peroxidase activity and a Chemidoc analyzer (Bio-Rad Laboratories, Hercules, CA) was used for detection. Membranes were reprobed with mouse anti-actin antibody and anti-mouse-HRP antibody to normalize between samples. Protein abundance was quantified using Image Lab software (Bio-Rad Laboratories, Hercules, CA).

4.11 | Protein degradation assays

After entrainment, seedlings were moved at dawn (ZT0) to constant darkness or constant 60 μmol m^{-2} s^{-1} monochromatic blue or red light under LEDs (XtremeLUX, Santa Clara, CA) at 22°C. During the day (ZT5 or ZT7) or subjective night (ZT17 or ZT19), seedlings were treated with cycloheximide by submerging them in liquid 1X Murashige and Skoog, 3% sucrose, and 200 uM cycloheximide on a shaker and collected 0, 1, 2, or 4 h later. Samples were prepared and quantified as previously described (Shalit-Kaneh et al., 2018), and western blotting and protein quantification were performed as described above.

4.12 | Statistical analysis and data visualization

All statistical analyses and data visualization were performed using R (R Core Team, 2021). Figures were generated using the tidyverse (Wickham et al., 2019), RColorBrewer (Neuwirth, 2014), cowplot (Wilke, 2020a), gridExtra (Auguie, 2017), glue (Hester & Bryan, 2022), and ggtext (Wilke, 2020b) packages. Gene models were created using the genemodel package (Monroe, 2017). Linear mixed-effect models were used in one-way ANOVA and Tukey's post hoc tests. To compare flowering time and rosette growth differences between genotypes within each condition (long day or short day), we used model "growth phenotype ~ genotype + (1|rep) + (1|flat)." To compare hypocotyl length differences between genotypes at each fluence rate, we used model "length ~ genotype + (1|rep)." To compare period phenotype differences between genotypes at each fluence rate, we used model "period ~ genotype + (1|rep)." Linear mixed-effect models were also used in two-way ANOVA and Tukey's post hoc tests. To compare the effect of fluence rate on circadian period between genotypes, we used model "period ~ genotype * fluence rate + (1|rep)." To compare the effect of fluence rate on hypocotyl length between genotypes, we used model "length ~ genotype * fluence rate + (1|rep)." Modeling was done with the lme4 (Bates et al., 2015) and lmerTest (Kuznetsova et al., 2017) packages; tests were performed using the lattice (Sarkar, 2008), broom (Robinson et al., 2021), and emmeans (Lenth, 2022) packages. Results were visualized with the multcomp (Hothorn et al., 2008) and multcompView (Graves et al., 2019) packages.

For protein degradation analysis, nonlinear Bayesian regressions were performed using the brms (Bürkner, 2017) package. We used an exponential decay model:

$$y \sim N_o * e^{-k*t},$$

where y = protein concentration at time t, N_0 = protein concentration at time 0, k = the protein degradation rate, and t = time. Depending on the analysis, coefficients for k and N_0 were fit to correspond to genotype, ZT, and their interaction, or to light color, ZT, and their interaction. We also evaluated models where random effects of experiment and replicate were included for k and N_o. Leave-one-out analysis was used for model selection, and the simplest model that was not significantly different from the best fit model was selected. Generally, the selected models did not retain any random effect terms. For details of this analysis, see scripts online (https://github.com/MaloofLab/Hughes-RVE-2023).

4.13 | Accession numbers

Accession numbers for *Arabidopsis thaliana* genes are referenced here:

CCA1 - AT4G16780
CRY2 - AT1G04400
ELF3 - AT2G25930
ELF4 - AT2G40080
HY5 - AT5G11260

LHY - AT1G01060
LUX - AT3G46640
PRR5 - AT3G59060
PRR7 - AT5G02810
PRR9 - AT2G46790
RVE4 - AT5G02840
RVE6 - AT5G52660
RVE8 - AT3G09600
TOC1 - AT5G61380
ZTL - AT5G57360

AUTHOR CONTRIBUTIONS

C. L. H., Y. A., and S. L. H. designed the project. C. L. H. and Y. A. performed the research. All authors analyzed data. C. L. H. and S. L. H. and wrote the manuscript with comments from Y. A. and J. N. M.

ACKNOWLEDGMENTS

This work was supported by an award from the National Institutes of Health (R01 GM069418) and the U.S. Department of Agriculture-National Institute of Food and Agriculture (CA-D-PLB-2259-H). We thank the members of the Harmer and Maloof labs for many helpful discussions and Hongtao Qian for assistance with hypocotyl length measurements.

CONFLICT OF INTEREST STATEMENT

The authors declare no conflict of interest associated with the work described in this manuscript.

DATA AVAILABILITY STATEMENT

The data that support the findings of this study are available from the corresponding author upon reasonable request.

ORCID

Cassandra L. Hughes https://orcid.org/0009-0004-7001-3250
Yuyan An https://orcid.org/0000-0002-2810-0252
Stacey L. Harmer https://orcid.org/0000-0001-6813-6682

REFERENCES

Adams, S., Grundy, J., Veflingstad, S. R., Dyer, N. P., Hannah, M. A., Ott, S., & Carré, I. A. (2018). Circadian control of abscisic acid biosynthesis and signalling pathways revealed by genome-wide analysis of LHY binding targets. *The New Phytologist*, *220*(3), 893–907. https://doi.org/10.1111/nph.15415

Alabadi, D., Oyama, T., Yanovsky, M. J., Harmon, G., Mas, P., & Kay, S. A. (2001). Reciprocal regulation between *TOC1* and *LHY/CCA1* within the *Arabidopsis* circadian clock. *Science*, *293*(5531), 880–883. https://doi.org/10.1126/science.1061320

Aschoff, J. (1979). Circadian rhythms: Influences of internal and external factors on the period measured in constant conditions. *Zeitschrift für Tierpsychologie*, *49*(3), 225–249. https://doi.org/10.1111/j.1439-0310.1979.tb00290.x

Auguie, B. (2017). gridExtra: Miscellaneous functions for "grid" graphics. https://CRAN.R-project.org/package=gridExtra

Bates, D., Mächler, M., Bolker, B., & Walker, S. (2015). Fitting linear mixed-effects models using lme4. *Journal of Statistical Software*, *67*(1), 1–48. https://doi.org/10.18637/jss.v067.i01

Bürkner, P. C. (2017). brms: An R package for Bayesian multilevel models using Stan. *Journal of Statistical Software*, *80*(1), 1–28. https://doi.org/10.18637/jss.v080.i01

Chen, H., Zhang, J., Neff, M. M., Hong, S. W., Zhang, H., Deng, X. W., & Xiong, L. (2008). Integration of light and abscisic acid signaling during seed germination and early seedling development. *Proceedings. National Academy of Sciences. United States of America*, *105*(11), 4495–4500. https://doi.org/10.1073/pnas.0710778105

Clough, S. J., & Bent, A. F. (1998). Floral dip: A simplified method for agrobacterium-mediated transformation of *Arabidopsis thaliana*. *The Plant Journal*, *16*(6), 735–743. https://doi.org/10.1046/j.1365-313x.1998.00343.x

Covington, M. F., Panda, S., Liu, X. L., Strayer, C. A., Wagner, D. R., & Kay, S. A. (2001). ELF3 modulates resetting of the circadian clock in Arabidopsis. *The Plant Cell*, *13*(6), 1305–1316. https://doi.org/10.1105/TPC.000561

Creux, N., & Harmer, S. (2019). Circadian rhythms in plants. *Cold Spring Harbor Perspectives in Biology*, *11*(9), a034611. https://doi.org/10.1101/cshperspect.a034611

Dodd, A. N., Salathia, N., Hall, A., Kévei, E., Tóth, Ŕ., Nagy, F., Hibberd, J. M., Millar, A. J., & Webb, A. A. R. (2005). Plant circadian clocks increase photosynthesis, growth, survival, and competitive advantage. *Science*, *309*(5734), 630–633. https://doi.org/10.1126/science.1115581

Farinas, B., & Mas, P. (2011). Functional implication of the MYB transcription factor *RVE8/LCL5* in the circadian control of histone acetylation. *The Plant Journal*, *66*(2), 318–329. https://doi.org/10.1111/j.1365-313X.2011.04484.x

Fujiwara, S., Wang, L., Han, L., Suh, S. S., Salomé, P. A., McClung, C. R., & Somers, D. E. (2008). Post-translational regulation of the Arabidopsis circadian clock through selective proteolysis and phosphorylation of pseudo-response regulator proteins. *The Journal of Biological Chemistry*, *283*(34), 23073–23083. https://doi.org/10.1074/jbc.M803471200

Gangappa, S. N., & Botto, J. F. (2016). The multifaceted roles of HY5 in plant growth and development. *Molecular Plant*, *9*(10), 1353–1365. https://doi.org/10.1016/j.molp.2016.07.002

Geng, F., & Tansey, W. P. (2012). Similar temporal and spatial recruitment of native 19S and 20S proteasome subunits to transcriptionally active chromatin. *Proceedings. National Academy of Sciences. United States of America*, *109*(16), 6060–6065. https://doi.org/10.1073/pnas.1200854109

Graves, S., Piepho, H. P., & Sundar Dorai-Raj, L. S. (2019). multcompView: Visualizations of paired comparisons . https://CRAN.R-project.org/package=multcompView

Gray, J. A., Shalit-Kaneh, A., Chu, D. N., Hsu, P. Y., & Harmer, S. L. (2017). The REVEILLE clock genes inhibit growth of juvenile and adult plants by control of cell size. *Plant Physiology*, *173*(4), 2308–2322. https://doi.org/10.1104/pp.17.00109

Guo, H., Yang, H., Mockler, T. C., & Lin, C. (1998). Regulation of flowering time by *Arabidopsis* photoreceptors. *Science*, *279*(5355), 1360–1363. https://doi.org/10.1126/science.279.5355.1360

Hajdu, A., Dobos, O., Domijan, M., Bálint, B., Nagy, I., Nagy, F., & Kozma-Bognár, L. (2018). ELONGATED HYPOCOTYL 5 mediates blue light signalling to the Arabidopsis circadian clock. *The Plant Journal*, *96*(6), 1242–1254. https://doi.org/10.1111/tpj.14106

Hartley, J. L., Temple, G. F., & Brasch, M. A. (2000). DNA cloning using in vitro site-specific recombination. *Genome Research*, *10*(11), 1788–1795. https://doi.org/10.1101/gr.143000

Hazen, S. P., Schultz, T. F., Pruneda-Paz, J. L., Borevitz, J. O., Ecker, J. R., & Kay, S. A. (2005). *LUX ARRHYTHMO* encodes a Myb domain protein essential for circadian rhythms. *Proceedings. National Academy of Sciences. United States of America*, *102*(29), 10387–10392. https://doi.org/10.1073/pnas.0503029102

He, Y., Yu, Y., Wang, X., Qin, Y., Su, C., & Wang, L. (2022). Aschoff's rule on circadian rhythms orchestrated by blue light sensor CRY2 and

clock component PRR9. *Nature Communications*, *13*(1), 5869. https://doi.org/10.1038/s41467-022-33568-3

Hester, J., & Bryan, J. (2022). glue: Interpreted string literals. https://CRAN.R-project.org/package=glue

Hothorn, T., Bretz, F., & Westfall, P. (2008). Simultaneous inference in general parametric models. *Biometrical Journal*, *50*(3), 346–363. https://doi.org/10.1002/bimj.200810425

Hsu, P. Y., Devisetty, U. K., & Harmer, S. L. (2013). Accurate timekeeping is controlled by a cycling activator in *Arabidopsis*. *eLife*, *2*, e00473. https://doi.org/10.7554/eLife.00473

Hsu, P. Y., & Harmer, S. L. (2014). Wheels within wheels: The plant circadian system. *Trends in Plant Science*, *19*(4), 240–249. https://doi.org/10.1016/j.tplants.2013.11.007

Hughes, C. L., & Harmer, S. L. (2023). Myb-like transcription factors have epistatic effects on circadian clock function but additive effects on plant growth. *Plant Direct*, *7*(10), e533. https://doi.org/10.1002/pld3.533

Kamioka, M., Takao, S., Suzuki, T., Taki, K., Higashiyama, T., Kinoshita, T., & Nakamichi, N. (2016). Direct repression of evening genes by CIRCADIAN CLOCK-ASSOCIATED1 in the Arabidopsis circadian clock. *The Plant Cell*, *28*(3), 696–711. https://doi.org/10.1105/tpc.15.00737

Kidokoro, S., Hayashi, K., Haraguchi, H., Ishikawa, T., Soma, F., Konoura, I., Toda, S., Mizoi, J., Suzuki, T., Shinozaki, K., & Yamaguchi-Shinozaki, K. (2021). Posttranslational regulation of multiple clock-related transcription factors triggers cold-inducible gene expression in *Arabidopsis*. *Proceedings. National Academy of Sciences. United States of America*, *118*(10), e2021048118. https://doi.org/10.1073/pnas.2021048118

Kuznetsova, A., Brockhoff, P. B., & Christensen, R. H. B. (2017). lmerTest package: Tests in linear mixed effects models. *Journal of Statistical Software*, *82*(13), 1–26. https://doi.org/10.18637/jss.v082.i13

Lenth, R. V. (2022). emmeans: Estimated marginal means, aka least-squares means. https://github.com/rvlenth/emmeans

Li, G., Siddiqui, H., Teng, Y., Lin, R., Wan, X. Y., Li, J., Lau, O. S., Ouyang, X., Dai, M., Wan, J., Devlin, P. F., Deng, X. W., & Wang, H. (2011). Coordinated transcriptional regulation underlying the circadian clock in *Arabidopsis*. *Nature Cell Biology*, *13*(5), 616–622. https://doi.org/10.1038/ncb2219

Lipford, J. R., & Deshaies, R. J. (2003). Diverse roles for ubiquitin-dependent proteolysis in transcriptional activation. *Nature Cell Biology*, *5*(10), 845–850. https://doi.org/10.1038/ncb1003-845

Locke, J. C. W., Southern, M. M., Kozma-Bognár, L., Hibberd, V., Brown, P. E., Turner, M. S., & Millar, A. J. (2005). Extension of a genetic network model by iterative experimentation and mathematical analysis. *Molecular Systems Biology*, *1*(1), 2005.0013. https://doi.org/10.1038/msb4100018

Maeda, A. E., & Nakamichi, N. (2022). Plant clock modifications for adapting flowering time to local environments. *Plant Physiology*, *190*(2), 952–967. https://doi.org/10.1093/plphys/kiac107

Maloof, J. N., Nozue, K., Mumbach, M. R., & Palmer, C. M. (2013). LeafJ: An ImageJ plugin for semi-automated leaf shape measurement. *JoVE*, *71*, e50028. https://doi.org/10.3791/50028

Mancini, E., Sanchez, S. E., Romanowski, A., Schlaen, R. G., Sanchez-Lamas, M., Cerdán, P. D., & Yanovsky, M. J. (2016). Acute effects of light on alternative splicing in light-grown plants. *Photochemistry and Photobiology*, *92*(1), 126–133. https://doi.org/10.1111/php.12550

Martin-Tryon, E. L., Kreps, J. A., & Harmer, S. L. (2007). *GIGANTEA* acts in blue light signaling and has biochemically separable roles in circadian clock and flowering time regulation. *Plant Physiology*, *143*(1), 473–486. https://doi.org/10.1104/pp.106.088757

Más, P., Devlin, P. F., Panda, S., & Kay, S. A. (2000). Functional interaction of phytochrome B and cryptochrome 2. *Nature*, *408*(6809), 207–211. https://doi.org/10.1038/35041583

Más, P., Kim, W. Y., Somers, D. E., & Kay, S. A. (2003). Targeted degradation of TOC1 by ZTL modulates circadian function in *Arabidopsis thaliana*. *Nature*, *426*(6966), 567–570. https://doi.org/10.1038/nature02163

Monroe, J. G. (2017). genemodel: Gene model plotting in R. https://github.com/greymonroe/genemodel

Muratani, M., & Tansey, W. P. (2003). How the ubiquitin–proteasome system controls transcription. *Nature Reviews. Molecular Cell Biology*, *4*(3), 192–201. https://doi.org/10.1038/nrm1049

Nagel, D. H., Doherty, C. J., Pruneda-Paz, J. L., Schmitz, R. J., Ecker, J. R., & Kay, S. A. (2015). Genome-wide identification of CCA1 targets uncovers an expanded clock network in *Arabidopsis*. *Proceedings. National Academy of Sciences. United States of America*, *112*(34), E4802–E4810. https://doi.org/10.1073/pnas.1513609112

Neuwirth, E. (2014). RColorBrewer: ColorBrewer palettes. https://CRAN.R-project.org/package=RColorBrewer

Oakenfull, R. J., & Davis, S. J. (2017). Shining a light on the Arabidopsis circadian clock. *Plant, Cell & Environment*, *40*(11), 2571–2585. https://doi.org/10.1111/pce.13033

Ouyang, Y., Andersson, C. R., Kondo, T., Golden, S. S., & Johnson, C. H. (1998). Resonating circadian clocks enhance fitness in cyanobacteria. *Proceedings. National Academy of Sciences. United States of America*, *95*(15), 8660–8664. https://doi.org/10.1073/pnas.95.15.8660

R Core Team. (2021). R: A language and environment for statistical computing. https://www.R-project.org/

Rawat, R., Takahashi, N., Hsu, P. Y., Jones, M. A., Schwartz, J., Salemi, M. R., Phinney, B. S., & Harmer, S. L. (2011). REVEILLE8 and PSEUDO-REPONSE REGULATOR5 form a negative feedback loop within the Arabidopsis circadian clock. *PLoS Genetics*, *7*(3), e1001350. https://doi.org/10.1371/journal.pgen.1001350

Robinson, D., Hayes, A., & Couch, S. (2021). broom: Convert statistical objects into tidy tibbles. https://CRAN.R-project.org/package=broom

Sanchez, S. E., Rugnone, M. L., & Kay, S. A. (2020). Light perception: A matter of time. *Molecular Plant*, *13*(3), 363–385. https://doi.org/10.1016/j.molp.2020.02.006

Sarkar, D. (2008). *Lattice: Multivariate data visualization with R*. Springer. https://doi.org/10.1007/978-0-387-75969-2

Schneider, C. A., Rasband, W. S., & Eliceiri, K. W. (2012). NIH image to ImageJ: 25 years of image analysis. *Nature Methods*, *9*(7), 671–675. https://doi.org/10.1038/nmeth.2089

Seluzicki, A., Burko, Y., & Chory, J. (2017). Dancing in the dark: Darkness as a signal in plants. *Plant, Cell & Environment*, *40*(11), 2487–2501. https://doi.org/10.1111/pce.12900

Shalit-Kaneh, A., Kumimoto, R. W., Filkov, V., & Harmer, S. L. (2018). Multiple feedback loops of the Arabidopsis circadian clock provide rhythmic robustness across environmental conditions. *Proceedings. National Academy of Sciences. United States of America*, *115*(27), 7147–7152. https://doi.org/10.1073/pnas.1805524115

Song, Y. H., Shim, J. S., Kinmonth-Schultz, H. A., & Imaizumi, T. (2015). Photoperiodic flowering: Time measurement mechanisms in leaves. *Annual Review of Plant Biology*, *66*(1), 441–464. https://doi.org/10.1146/annurev-arplant-043014-115555

Spoelstra, K., Wikelski, M., Daan, S., Loudon, A. S. I., & Hau, M. (2016). Natural selection against a circadian clock gene mutation in mice. *Proceedings. National Academy of Sciences. United States of America*, *113*(3), 686–691. https://doi.org/10.1073/pnas.1516442113

Wickham, H., Averick, M., Bryan, J., Chang, W., McGowan, L., François, R., Grolemund, G., Hayes, A., Henry, L., Hester, J., Kuhn, M., Pedersen, T., Miller, E., Bache, S., Müller, K., Ooms, J., Robinson, D., Seidel, D., Spinu, V., … Yutani, H. (2019). Welcome to the tidyverse. *J Open Source Softw.*, *4*(43), 1686. https://doi.org/10.21105/joss.01686

Wilke, C. O. (2020a). cowplot: Streamlined plot theme and plot annotations for ggplot2. https://wilkelab.org/cowplot/

Wilke, C. O. (2020b). ggtext: Improved text rendering support for ggplot2. https://wilkelab.org/ggtext/

Xiao, Y., Chu, L., Zhang, Y., Bian, Y., Xiao, J., & Xu, D. (2022). HY5: A pivotal regulator of light-dependent development in higher plants. *Frontiers in Plant Science*, *12*, 12. https://doi.org/10.3389/fpls.2021.800989

Yan, T., Heng, Y., Wang, W., Li, J., & Deng, X. W. (2022). SWELLMAP 2, a phyB-interacting splicing factor, negatively regulates seedling photomorphogenesis in Arabidopsis. *Frontiers in Plant Science*, *13*, 13. https://doi.org/10.3389/fpls.2022.836519

Zhai, Q., Yan, L., Tan, D., Chen, R., Sun, J., Gao, L., Dong, M. Q., Wang, Y., & Li, C. (2013). Phosphorylation-coupled proteolysis of the transcription factor MYC2 is important for jasmonate-signaled plant immunity. *PLoS Genetics*, *9*(4), e1003422. https://doi.org/10.1371/journal.pgen.1003422

Zielinski, T., Moore, A. M., Troup, E., Halliday, K. J., & Millar, A. J. (2014). Strengths and limitations of period estimation methods for circadian data. *PLoS ONE*, *9*(5), e96462. https://doi.org/10.1371/journal.pone.0096462

SUPPORTING INFORMATION

Additional supporting information can be found online in the Supporting Information section at the end of this article.

How to cite this article: Hughes, C. L., An, Y., Maloof, J. N., & Harmer, S. L. (2024). Light quality-dependent roles of REVEILLE proteins in the circadian system. *Plant Direct*, *8*(3), e573. https://doi.org/10.1002/pld3.573